

## Role of single-qubit decoherence time in adiabatic quantum computation

M. H. S. Amin,<sup>1</sup> C. J. S. Truncik,<sup>1</sup> and D. V. Averin<sup>2</sup>

<sup>1</sup>*D-Wave Systems Inc., 100-4401 Still Creek Drive, Burnaby, British Columbia, Canada V5C 6G9*

<sup>2</sup>*Department of Physics and Astronomy, SUNY Stony Brook, Stony Brook, New York 11794, USA*

(Received 2 May 2008; revised manuscript received 16 December 2008; published 4 August 2009)

We have studied numerically the evolution of an adiabatic quantum computer in the presence of a Markovian Ohmic environment by considering Ising spin-glass systems with up to 20 qubits independently coupled to this environment via two conjugate degrees of freedom. The required computation time is demonstrated to be of the same order as that for an isolated system and is not limited by the single-qubit decoherence time  $T_2^*$ , even when the minimum gap is much smaller than the temperature and decoherence-induced level broadening. For small minimum gap, the system can be described by an effective two-state model coupled only longitudinally to environment.

DOI: [10.1103/PhysRevA.80.022303](https://doi.org/10.1103/PhysRevA.80.022303)

PACS number(s): 03.67.Lx, 03.65.Yz

Adiabatic quantum computation [1] (AQC) is an attractive model of quantum computation (QC). It eliminates the need for precise timing of the qubit transformations required in the gate-model computation scheme and is also expected to possess some degree of fault tolerance afforded by the energy gap separating the ground from excited states of the qubit Hamiltonian. AQC approach is particularly appealing in the context of superconducting qubits which in principle have the required flexibility for implementation of complicated interactions. In the AQC, a system starts from a readily accessible ground state of some initial Hamiltonian  $H_i$  and slowly evolves into the ground state of the final Hamiltonian  $H_f$  which encodes a solution to the problem of interest:

$$H_S(t) = [1 - s(t)]H_i + s(t)H_f, \quad (1)$$

where  $s(t) \in [0, 1]$  is a monotonic function of time  $t$ . Here, we only consider a linear time sweep  $s(t) = t/t_f$ , where  $t_f$  is the total evolution time. Transitions out of the ground state can be caused by the Landau-Zener processes [2] at the anticrossing ( $s = s^*$ ), where the gap  $g$  between the ground state  $|0\rangle$  and first excited state  $|1\rangle$  goes through a minimum:  $g_m \equiv g(s^*)$ . The probability of being in the ground state at the end of the adiabatic evolution is approximately ( $\hbar = k_B = 1$ )

$$P_{0f} = 1 - e^{-t_f/t_a}, \quad t_a \equiv \frac{4}{\pi g_m^2} \left\langle 1 \left| \frac{dH_S}{ds} \right| 0 \right\rangle_{s=s^*}. \quad (2)$$

To ensure large  $P_{0f}$ , one needs  $t_f \gtrsim t_a$ . The computation time is hence determined by  $t_a$  and thus by  $g_m$ .

In the gate-model QC, there is no direct correspondence between the wave function and the instantaneous system Hamiltonian. The Hamiltonian is only applied at the time of gate operations and usually involves only a few qubits. The wave function, therefore, is strongly affected by the environment and is irreversibly altered after the decoherence time, which is typically smaller than the single-qubit dephasing time  $T_2^*$ . This means that  $T_2^*$  imposes an upper limit on the total computation time, unless some quantum error correction scheme (which requires significant resources) is utilized. This is not true for AQC, as the wave function is always very close to the instantaneous ground state of the system Hamiltonian and is consequently more stable against the decoher-

ence. Qualitatively, one expects decoherence to drive the system's reduced density matrix toward being diagonal in the energy basis, which is not harmful for AQC but is detrimental for the gate-model QC. Such robustness has been demonstrated in previous studies [3–10]. However, those studies have either used a two-state model to describe the behavior of a multilevel system at the anticrossing or assumed noise models that are not motivated by physical implementations. In this paper, we numerically study quantum evolution of a multiqubit system directly without the two-state approximation, assuming a quite general and realistic coupling to environment.

We consider a very general Hamiltonian  $H(t) = H_S(t) + H_B + H_{\text{int}}$ , which includes system, bath, and interaction between them, respectively. The dynamics of the total (system plus environment) density matrix is governed by the Liouville equation [11]:  $\dot{\rho}(t) = -i[H(t), \rho(t)]$ . The reduced density matrix for the system is obtained by partially tracing over the environmental degrees of freedom:  $\rho_S = \text{Tr}_B[\rho]$ . Let  $|n(t)\rangle$  denote the instantaneous eigenstates of the system Hamiltonian:  $H_S(t)|n(t)\rangle = E_n(t)|n(t)\rangle$ . In this basis, we define  $\rho_{nm}(t) = \langle n(t)|\rho_S(t)|m(t)\rangle$ . Taking the time derivative, we obtain (dropping explicit time dependences)

$$\dot{\rho}_{nm} = \langle n|\dot{\rho}_S|m\rangle + \langle \dot{n}|\rho_S|m\rangle + \langle n|\rho_S|\dot{m}\rangle. \quad (3)$$

We begin by focusing on the first term in Eq. (3) which is responsible for the decay processes. We treat it quasistatically, assuming that the evolution of the Hamiltonian is much slower than the environmentally induced decay rates, so that the eigenstates can be taken as time independent. We also assume that the effect of the system on the environment is so small that the bath maintains its equilibrium distribution  $\rho_B$  at all times. Moreover, the bath is taken to have correlation time  $\tau_B$  shorter than all the decay times of the system so that one can apply Markovian approximation. Then, using the standard Bloch-Redfield formalism, one can show that [11,12]

$$\begin{aligned} \langle n|\dot{\rho}_S|m\rangle &= -i\omega_{nm}\rho_{nm} + e^{-i\omega_{nm}t}\langle n|\dot{\rho}_S|m\rangle \\ &= -i\omega_{nm}\rho_{nm} - \sum_{k,l} R_{nmkl}\rho_{kl}, \end{aligned} \quad (4)$$

where  $\omega_{nm} = E_n - E_m$ , and

$$R_{nmkl} = \delta_{lm}\Gamma_{nrk}^{(+)} + \delta_{nk}\Gamma_{lrm}^{(-)} - \Gamma_{lmnk}^{(+)} - \Gamma_{lmnk}^{(-)},$$

$$\Gamma_{lmnk}^{(+)} = \int_0^\infty dt e^{-i\omega_{nk}t} \langle \tilde{H}_{l,lm}(t) \tilde{H}_{l,nk}(0) \rangle, \quad (5)$$

$$\Gamma_{lmnk}^{(-)} = \int_0^\infty dt e^{-i\omega_{lm}t} \langle \tilde{H}_{l,lm}(0) \tilde{H}_{l,nk}(t) \rangle,$$

$$\tilde{H}_{l,lm}(t) = \langle n | e^{iH_B t} H_{\text{int}}(t) e^{-iH_B t} | m \rangle. \quad (6)$$

Here,  $\langle \dots \rangle \equiv \text{Tr}_B[\rho_B \dots]$ , and summation over repeated indices is implied in Eq. (5).

Substituting Eq. (4) into Eq. (3), we obtain

$$\dot{\rho}_{nm} = -i\omega_{nm}\rho_{nm} - \sum_{k,l} (R_{nmkl} - M_{nmkl})\rho_{kl}, \quad (7)$$

where  $M_{nmkl} = \delta_{nk}\langle l | \dot{m} \rangle + \delta_{ml}\langle \dot{n} | k \rangle$ . The tensors  $M_{nmkl}$  and  $R_{nmkl}$  are responsible for nonadiabatic and thermal transitions, respectively. For a time-independent Hamiltonian,  $M_{nmkl} = 0$ , and Eq. (7) becomes the Bloch-Redfield equations [11,12]. The derivatives like  $|\dot{n}\rangle$  can be calculated numerically. It is important to ensure that the equation stays trace preserving, which requires  $\text{Re} \sum_{n,m} \langle n | \dot{m} \rangle = 0$ . This condition is *exactly* satisfied (even with the truncation discussed below), if we write  $\langle n(t) | \dot{m}(t) \rangle = \frac{1}{4\delta t} \{ \langle n(t+\delta t) | + \langle n(t-\delta t) | \} \{ |m(t+\delta t)\rangle - |m(t-\delta t)\rangle \}$ .

To introduce coupling to environment, we consider a quite general interaction Hamiltonian

$$H_{\text{int}} = - \sum_{i=1}^n (Q_x^{(i)} \sigma_x^{(i)} + Q_z^{(i)} \sigma_z^{(i)}), \quad (8)$$

where  $\sigma_{x,z}^{(i)}$  are the Pauli matrices of the  $i$ th qubit and  $Q_\alpha^{(i)}$  are the heat-bath operators. Using Eq. (6), and assuming uncorrelated heat baths, we find

$$\Gamma_{lmnk}^{(+)} = \frac{1}{2} \sum_{i,\alpha} S_\alpha^{(i)}(-\omega_{nk}) \sigma_{\alpha,lm}^{(i)} \sigma_{\alpha,nk}^{(i)},$$

$$\Gamma_{lmnk}^{(-)} = \frac{1}{2} \sum_{i,\alpha} S_\alpha^{(i)}(\omega_{lm}) \sigma_{\alpha,lm}^{(i)} \sigma_{\alpha,nk}^{(i)}, \quad (9)$$

where  $S_\alpha^{(i)}(\omega) = \int_{-\infty}^\infty dt e^{i\omega t} \langle Q_\alpha^{(i)}(t) Q_\alpha^{(i)}(0) \rangle$  are the bath spectral densities and  $\sigma_{\alpha,lm}^{(i)} = \langle l | \sigma_\alpha^{(i)} | m \rangle$ . Here, we have neglected the imaginary parts of  $\Gamma_{lmnk}^{(\pm)}$ , as they only produce small shifts of energies which in principle can be accounted for by proper renormalization.

To model the spectral densities, we assume Ohmic bosonic heat baths in thermal equilibrium [13]:  $S_\alpha^{(i)}(\omega) = \eta_\alpha^{(i)} \omega e^{-|\omega|/\omega_c} / (1 - e^{-\omega/T})$ . The dimensionless coefficients  $\eta_\alpha^{(i)}$  describe the strength of coupling between the qubits and environment and  $\omega_c$  is a cutoff frequency which we assume to be larger than all relevant energy scales. The Markovian approximation is valid as long as  $\tau_B \sim 1/\omega_c$  is shorter than all the decay times and the characteristic time variation of the Hamiltonian.

We now use the above model to study the evolution of a

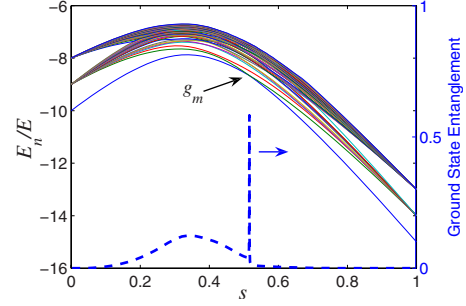


FIG. 1. (Color online) Energy spectrum for a 20-qubit instance with a very small minimum gap:  $g_m/E \approx 5 \times 10^{-4}$ . Only the first 50 energy levels of the total  $\sim 10^6$  are shown. The dashed line in the bottom represents the ground-state entanglement calculated using Meyer and Wallach entanglement measure (12).

multiqubit Ising system with the initial and final Hamiltonians given by

$$\frac{H_i}{E} = -\frac{1}{2} \sum_i \Delta_i \sigma_x^{(i)}, \quad (10)$$

$$\frac{H_f}{E} = -\frac{1}{2} \sum_i h_i \sigma_z^{(i)} + \frac{1}{2} \sum_{i>j} J_{ij} \sigma_z^{(i)} \sigma_z^{(j)}, \quad (11)$$

where  $\Delta_i$ ,  $h_i$ , and  $J_{ij}$  are dimensionless parameters and  $E$  is an energy scale. We consider square lattice configurations with nearest- and next-nearest-neighbor couplings between the qubits. The choice of only two-qubit short-range interactions is motivated by the feasibility of experimental implementation. We generate spin-glass instances involving 6, 9, 12, 16, and 20 qubits by randomly choosing  $h_i$  and  $J_{ij}$  from  $\{-1, 0, 1\}$  and identifying small gap instances with nondegenerate final ground state (see, e.g., Fig. 1). Such instances are very rare and represent difficult problems; a degenerate ground state (multiple solutions) ensures higher probability of finding one of the solutions. We also choose  $\Delta_i = 1$  for all  $i$ .

Figure 1 shows the energy spectrum for a 20-qubit instance with a very small  $g_m$ . The first two energy levels anticross near the middle of the evolution. We should mention that this is not a typical 20-qubit spectrum for the problem we consider. Indeed for an average problem the minimum gap is much larger and instances with such a small gap are very rare. For such instances, the bottleneck of the adiabatic evolution is expected to be near the anticrossing. Moreover, since the gap is much smaller than the typical energy separation of the levels, two-state approximation is expected to be sufficient to describe the evolution. This can be tested by comparing a fully numerical simulation without two-state approximation with a two-state model, which will be done at the end of this paper.

To study the evolution, we numerically integrate Eq. (7) starting from  $\rho_S(0) = |0\rangle\langle 0|$ . For large number of qubits, the computation becomes extremely time consuming because of the large number of matrix elements in  $\rho_S$ . However, since  $\rho_S$  is written in the energy basis at all times, it is possible to significantly simplify the computation by truncating  $\rho_S$  to

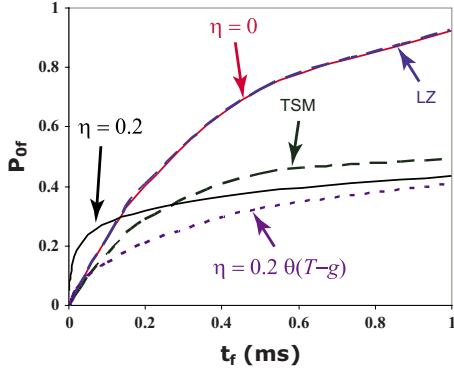


FIG. 2. (Color online) Probability of success  $P_{of}$  as a function of  $t_f$  for the 20-qubit instance of Fig. 1. The solid lines are calculated with ( $\eta=0.2$ ) and without ( $\eta=0$ ) coupling to the environment. Other parameters are  $E=10$  GHz and  $T=25$  mK. The case without coupling to the environment is compared with the pure Landau-Zener behavior using Eq. (2) (see dashed blue line marked by LZ). The excellent agreement confirms that for the coherent evolution, the two-state model is sufficient to calculate the probability. The (black) dashed line, marked by TSM, is obtained using analytical formula (17) obtained using a two-state model. It asymptotically shows the same behavior as the numerical result (solid line marked by  $\eta=0.2$ ). The dotted line is numerical calculation with  $\eta=0.2\theta(T-g)$ , which eliminates relaxation after the anticrossing (see the text for description).

only the lowest few energy levels occupied in the course of evolution. To ensure small error, we increase the number of levels kept in the calculation until the results do not change. Typically maximum 7–8 energy levels are sufficient for the type of evolution and instances we consider here. For very slow evolutions, even two states suffice to achieve acceptable accuracy. The numerical integration time can also be significantly reduced by refining the integration steps based on the gap size.

Figure 2 shows the probability of staying in the ground state at the end of the evolution as a function of  $t_f$  for the 20-qubit instance depicted in Fig. 1. For simplicity, we have chosen the same coupling to the environment for all qubits:  $\gamma_\alpha^{(i)} = \eta$ . Notice that with the chosen parameters, the minimum energy gap is much smaller than temperature ( $g_m/T \approx 10^{-2}$ ), hence thermal excitation at the anticrossing is expected. For a closed system ( $\eta=0$ ) the numerics agree very well with Eq. (2). For an open system ( $\eta=0.2$ ), however, the probability is enhanced (compared to the closed system) at small  $t_f$ , while it is suppressed for large  $t_f$ , asymptotically approaching its equilibrium value. Therefore, it is more efficient to run the system for a shorter time and repeat the process than to wait for a long time to attain significant probability. An important point is that the time scale for the probabilities to reach some nonvanishing value is almost the same ( $\sim 1$  ms) for all curves. This has been a generic property for all instances that we have studied regardless of the size of the gap.

The thermally assisted behavior in short  $t_f$  regime is the result of large relaxation after the anticrossing region and is not expected to enhance the scaling of the computation [8]. To confirm this, we have repeated the numerical calculations,

but now allowing transitions only in the thermal mixing region by choosing  $\eta=0.2\theta(T-g)$ . This type of coupling coefficient only allows thermalization in a region with  $g < T$  and therefore eliminates the relaxation back to the ground state after the anticrossing. The result (dotted line in Fig. 2) shows no initial enhancement compared to the closed system, confirming the above statement.

We now compare the numerically calculated computation time with the single-qubit decoherence times. If the qubits are uncoupled ( $J_{ij}=0$ ), the single-qubit decoherence rates, in weak coupling limit, are given by  $1/T_2^* \sim S_\alpha^{(i)}(0) \sim \eta T$ . For the parameters of Fig. 2,  $T_2^* \sim 10$  ns, which is typical for solid-state qubits. This decoherence time is five orders of magnitude smaller than the computation time ( $\sim 1$  ms) for the problem of Fig. 2. Therefore, unlike the gate model QC, in AQC, the computation time is not limited by the single-qubit decoherence time.

It should be noted that the qubits will go through an entangled state during the evolution. To demonstrate that, we have displayed in Fig. 1 the ground-state entanglement (dashed line) calculated using the measure originally proposed by Meyer and Wallach [14]:

$$Q(|\psi\rangle) = \frac{1}{n} \sum_{k=1}^n 2(1 - \text{Tr}[\rho_k^2]), \quad (12)$$

where  $\rho_k \equiv \text{Tr}_{j \neq k} |\psi\rangle\langle\psi|$  is obtained by partially tracing over all qubits except the  $k$ th one. The ground-state entanglement becomes nonzero in the first half of the evolution with a very sharp peak at the anticrossing. The measure (12), however, does not describe quantitatively the actual (mixed-state) entanglement at that point, since it does not account for thermal mixing. Unfortunately, no practical mixed-state entanglement measure exists for more than two qubits [15]. The entanglement will not be destroyed by the environment (except maybe at the anticrossing) as long as the system dominantly populates the ground state. Therefore, despite the fact that the evolution time is far beyond the qubits' dephasing time, the system still preserves its quantum-mechanical behavior throughout the evolution. Once again, this is in contrast to what is expected in the gate-model QC. Qualitative demonstration of the nonvanishing ground-state entanglement during the evolution is also important as it shows that the evolution cannot be described efficiently in only classical terms.

The numerical method presented here is valid only for a Markovian environment. Most environments, however, especially in superconducting systems, are not Markovian and have a significant amount of low frequency noise. In Ref. [10], we have used the two-state model (TSM) approximation to study the effect of a non-Markovian environment on AQC. For the rest of this paper, we focus on showing that the TSM is adequate for the description of the AQC performance in the small-gap regime. For the environment to be able to cause transitions out of the ground state, the interaction Hamiltonian should have nonzero matrix elements between the ground state and the target state. We introduce

$$M_\alpha = \left( \frac{1}{n} \sum_i |\sigma_{\alpha,10}^{(i)}|^2 \right)^{1/2} \quad (13)$$

which give the rms values of the matrix elements of Pauli matrices  $\sigma_\alpha^{(i)}$  between the lowest two states. They represent

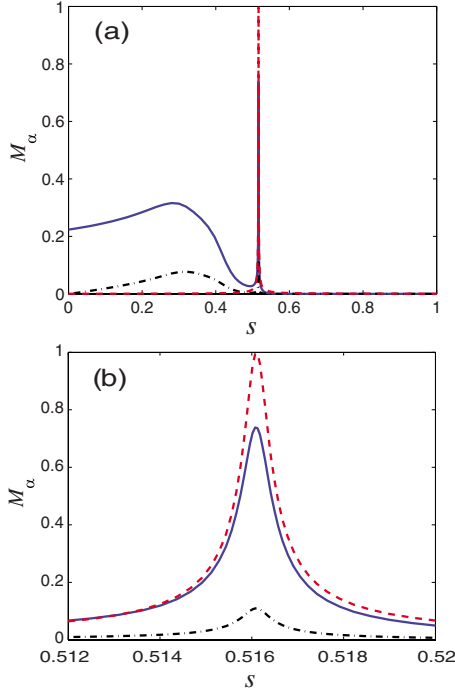


FIG. 3. (Color online) (a) The rms value of the matrix elements of the Pauli matrices between the first two states as defined in Eq. (13). Solid (blue) line is  $M_z$ ; dashed-dotted (black) line is  $M_x$ . We have also plotted the matrix element ( $M_z^{\text{TSM}}$ ) of  $\tau_z$  between the two energy levels of a two-state model described by Hamiltonian (15). (b) The same curves zoomed near the anticrossing show qualitative agreement (except for a prefactor) between all three curves.

some average behavior of the corresponding matrix elements and are closely related to relaxation between the two levels. Especially, if all the qubits have the same coupling  $\eta$  to the environment, the relaxation rate between the two states is given by

$$\gamma = n(M_x^2 + M_z^2)\tilde{S}(\omega_{10}), \quad (14)$$

where  $\tilde{S}(\omega)$  is the symmetrized spectral density of the (uncorrelated) baths. Figure 3(a) displays  $M_x$  and  $M_z$  as a function of  $s$  for the 20-qubit system of Fig. 1. Except for the initial region, they both show the same behavior: a sharp peak at the anticrossing, with a width proportional to  $g_m$ , followed by a vanishingly small value. For small  $T$ , the excitation from the ground state will be suppressed everywhere except near the anticrossing, where  $g < T$ .

The transitions at the anticrossing can be described by an effective two-state Hamiltonian:

$$H_S^{\text{TSM}} = -\frac{1}{2}(g_m\tau_x + \epsilon\tau_z),$$

$$H_{\text{int}}^{\text{TSM}} = -(Q_x^{\text{TSM}}\tau_x + Q_z^{\text{TSM}}\tau_z), \quad (15)$$

where  $\tau_\alpha$  are the Pauli matrices in the two-state subspace,  $\epsilon = 2\tilde{E}(s - s^*)$ , with  $s^*$  being the position of the anticrossing and  $\tilde{E}$  an energy scale (in our case, close to  $E$ ) characterizing the anticrossing. We introduce the matrix elements

$$M_x^{\text{TSM}} = |\langle 0 | \tau_x | 1 \rangle| = |\cos \theta|,$$

$$M_z^{\text{TSM}} = |\langle 0 | \tau_z | 1 \rangle| = |\sin \theta|, \quad (16)$$

which are responsible for the transitions between the two levels, where  $\tan \theta = g_m / \epsilon$ . Except for an overall factor,  $M_z^{\text{TSM}}$  has the same shape as both  $M_{x,z}$  (see the inset of Fig. 3), while  $M_x^{\text{TSM}}$  is completely different; it has a sharp dip at  $\epsilon = 0$  where it vanishes. Thus, in order for the effective two-state model to give the same result as the full system, it needs to couple to the environment only via  $\tau_z$  (i.e.,  $Q_x^{\text{TSM}} = 0$ ). In other words, a generic single-qubit coupling to the environment reduces to only longitudinal coupling in the effective TSM. Besides the numerical agreement, the fact that  $Q_x^{\text{TSM}} = 0$  in the two-state model has a deep physical meaning. As is clear in Eq. (16),  $M_x^{\text{TSM}} \approx 1$  everywhere except for a very small region near the anticrossing. In the presence of a nonvanishing  $Q_x^{\text{TSM}}$ , the relaxation rate will be very large almost everywhere and therefore the system should relax to the ground state in constant time even when  $s = 1$ . This is obviously unphysical and especially not expected for spin glasses for which the relaxation time to the ground state is extremely long. In the appendix of Ref. [9], the effective Hamiltonian (15) is systematically derived for the case of adiabatic Grover search problem [16]. For that problem, one finds  $Q_x^{\text{TSM}} = O(1/\sqrt{N})$ , but  $Q_z^{\text{TSM}} = O(1)$ , and therefore in large  $N$  limit the former vanishes in agreement with our physical expectation. Notice that in this case, the relaxation rate due to coupling of the bath to  $\tau_x$  is  $\gamma \propto (Q_x^{\text{TSM}})^2 = O(1/N)$ , therefore solving the problem merely based on relaxation leads to a computation time  $t_f = O(N)$ , which is the complexity of classical computation.

From the TSM Hamiltonian (15) with this type of longitudinal coupling, the success probability in the large- $T$  limit is [8,10]

$$P_{0f}^{\text{TSM}} = \frac{1}{2}(1 - e^{-2t_f/t_a}). \quad (17)$$

This formula is also plotted in Fig. 2. The qualitative asymptotic agreement with other numerical curves in the figure indicates that most of the transitions occur in the small-gap region ( $g \ll T$ ) where the TSM is adequate for their description.

To summarize, by studying spin-glass instances of up to 20 qubits (only one is illustrated), we have explicitly demonstrated that the computation time in AQC can be much longer than the single-qubit decoherence time  $T_2^*$ . In the case of small minimum gap (i.e., hard instances), effective two-state model with only the longitudinal coupling to environment describes transitions at the anticrossing. The numerical results also show that the computation time scale is unaffected by Ohmic environment. This conclusion cannot be understood directly as suppression of transitions to the excited states by the energy gap, since in the chosen instances it was much smaller at the anticrossing than the temperature and decoherence strength. Rather, it arises from the balance

of transitions between the two lowest levels. It should be emphasized that these results were obtained under the assumption of weak coupling to the environment, for which the discrete energy structure of  $H_S$  is mostly preserved. In the case of strong coupling, the interaction Hamiltonian would

dominate, and both the method and the conclusions of this work would not hold.

The authors are grateful to A. J. Berkley, P. Bunyk, V. Choi, R. Harris, J. Johansson, M. W. Johnson, T. M. Lanting, S. Lloyd, and G. Rose for useful discussions.

- 
- [1] E. Farhi, J. Goldstone, S. Gutmann, J. Lapan, A. Lundgren, and D. Preda, *Science* **292**, 472 (2001).
- [2] L. D. Landau, *Phys. Z. Sowjetunion* **2**, 46 (1932); C. Zener, *Proc. R. Soc. London, Ser. A* **137**, 696 (1932).
- [3] M. S. Sarandy and D. A. Lidar, *Phys. Rev. A* **71**, 012331 (2005); *Phys. Rev. Lett.* **95**, 250503 (2005).
- [4] A. M. Childs, E. Farhi, and J. Preskill, *Phys. Rev. A* **65**, 012322 (2001).
- [5] J. Roland and N. J. Cerf, *Phys. Rev. A* **71**, 032330 (2005).
- [6] M. Tiersch and R. Schützhold, *Phys. Rev. A* **75**, 062313 (2007).
- [7] S. Ashhab, J. R. Johansson, and F. Nori, *Phys. Rev. A* **74**, 052330 (2006).
- [8] M. H. S. Amin, P. J. Love, and C. J. S. Truncik, *Phys. Rev. Lett.* **100**, 060503 (2008).
- [9] A. T. S. Wan, M. H. S. Amin, and S. X. Wang, *Int. J. Quantum Inf.* **7**, 725 (2009).
- [10] M. H. S. Amin, D. V. Averin, and J. A. Nesteroff, *Phys. Rev. A* **79**, 022107 (2009).
- [11] K. Blum, *Density Matrix Theory and Applications*, 1st ed. (Plenum Publishing Corp., New York, 1981).
- [12] U. Weiss, *Quantum Dissipative Systems*, 2nd ed. (World Scientific, Singapore, 1999).
- [13] A. J. Leggett *et al.*, *Rev. Mod. Phys.* **59**, 1 (1987).
- [14] D. A. Meyer and N. R. Wallach, *J. Math. Phys.* **43**, 4273 (2002).
- [15] W. K. Wootters, *Phys. Rev. Lett.* **80**, 2245 (1998).
- [16] J. Roland and N. J. Cerf, *Phys. Rev. A* **65**, 042308 (2002).